



OPEN

DATA DESCRIPTOR

# Size-fractionated microbiome observed during an eight-month long sampling in Jiaozhou Bay and the Yellow Sea

Jianchang Tao<sup>1,2,3</sup>, Wenxiu Wang<sup>1,2,3</sup>, JL Weissman<sup>4</sup>, Yongyu Zhang<sup>5</sup>, Songze Chen<sup>1,2,3</sup>, Yuanqing Zhu<sup>1,3</sup>, Chuanlun Zhang<sup>1,2,3</sup> & Shengwei Hou<sup>1,2,6</sup>✉

Jiaozhou Bay is a typical semi-enclosed bay with a temperate climate imposed by strong anthropogenic influence. To investigate microbial biodiversity and ecosystem services in this highly dynamic coastal environment, we conducted a monthly microbial survey spanning eight months at two stations in the bay and the open Yellow Sea starting in April 2015. This report provides a comprehensive inventory of amplicon sequences and environmental microbial genomes from this survey. In total, 2,543 amplicon sequence variants were obtained with monthly relative abundance profiles in three size fractions (>2.7  $\mu\text{m}$ , 2.7–0.7  $\mu\text{m}$ , and 0.7–0.22  $\mu\text{m}$ ). Shotgun metagenomes yielded 915 high-quality metagenome-assembled genomes with  $\geq 50\%$  completeness and  $\leq 5\%$  contamination. These environmental genomes comprise 27 bacterial and 5 archaeal phyla. We expect this comprehensive dataset will facilitate a better understanding of coastal microbial ecology.

## Background & Summary

The global importance of microorganisms in biogeochemical cycling and climate change has been widely recognized<sup>1</sup>. Microbes play a central role in the marine food web by mediating carbon flow to upper trophic levels<sup>2</sup>, and are proposed to be responsible for the massive accumulation of recalcitrant dissolved organic carbon (rDOC) in the global ocean<sup>3,4</sup>. Seawater contains a contiguous body of particles, which have a predominant influence on microbial community assemblages. For instance, microbial community composition on particles was found to be consistently similar throughout the water column on a global scale<sup>5</sup>, and the size of particles may also play an important role in shaping microbial assemblage and community functioning<sup>6</sup>.

Particle niche partitioning suggests different trophic strategies. Free-living microbial communities are repeatedly observed to be distinct from particle-associated assemblages in both epipelagic<sup>7–9</sup> and bathypelagic oceans<sup>10,11</sup>. Microbes colonizing particles were found to be phylogenetically conserved<sup>11</sup> and metabolically more active than free-living ones<sup>12,13</sup>. Although there are plenty of studies showing that the rapid community response to particulate organic matters or nutrients is frequently associated with an altered microbial life strategy<sup>14–17</sup>, it is also evident that ecological interactions can complicate the interpretation<sup>18</sup>, particularly at finer phylogenetic resolutions<sup>19</sup>. Thus, it would be desirable to gain a better understanding of microbial particle association in both evolutionary and ecological aspects.

Coastal and estuarine environments are dynamic systems suffering from multiple anthropogenic stresses. Jiaozhou Bay (JZB) is such a typical semi-enclosed inlet of the Yellow Sea under strong and long-lasting human

<sup>1</sup>Shenzhen Key Laboratory of Marine Archaea Geo-Omics, Department of Ocean Science and Engineering, Southern University of Science and Technology, Shenzhen, 518000, China. <sup>2</sup>Southern Marine Science and Engineering Guangdong Laboratory (Guangzhou), Guangzhou, 511458, China. <sup>3</sup>Shanghai Sheshan National Geophysical Observatory, Shanghai Earthquake Agency, Shanghai, 200062, China. <sup>4</sup>Department of Biological Sciences-Marine and Environmental Biology, University of Southern California, Los Angeles, CA, 90089, USA. <sup>5</sup>Research Center for Marine Biology and Carbon Sequestration, Shandong Provincial Key Laboratory of Energy Genetics, Qingdao Institute of Bioenergy and Bioprocess Technology, Chinese Academy of Sciences, Qingdao, 266000, China. <sup>6</sup>State Key Laboratory for Marine Environmental Science, Institute of Marine Microbes and Ecospheres, Xiamen University, Xiamen, 361102, China. ✉e-mail: [housw@sustech.edu.cn](mailto:housw@sustech.edu.cn)

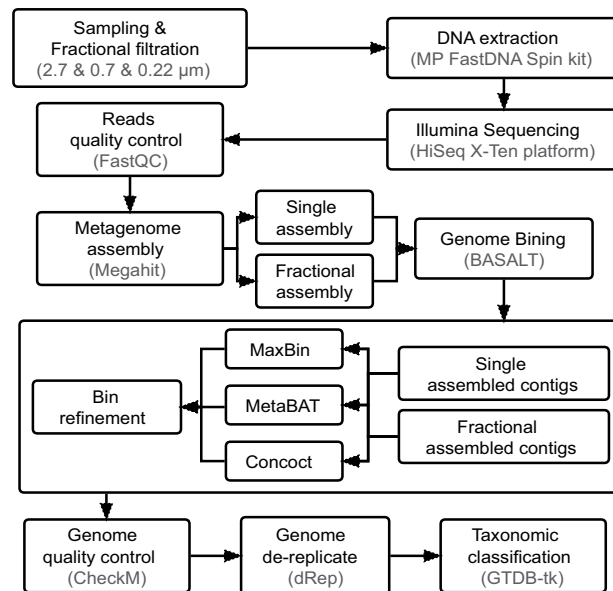


**Fig. 1** Bioinformatics workflow for amplicon and metagenomic data analysis. After sampling and filtration, microbial genomic DNA was extracted and libraries were prepared for amplicon and metagenomic sequencing. For amplicon data analysis, reads were quality controlled, denoised, and clustered using plugins of the QIIME2 suite. For metagenomic data analysis, preliminary MAGs were obtained after read quality control, metagenomic assembly and binning, then subjected to genome refinement and dereplication. The final MAGs were taxonomically classified and were used for further analysis. Detailed data processing steps, software, and parameters can be found in the Methods section.

impact. Substantial allochthonous organic matter is transported into the bay via several adjoining rivers, in addition to particles and pollutants released by a broad range of marine aquaculture farms<sup>20,21</sup>, causing eutrophication and frequent seasonal algal blooms in the past decades<sup>22</sup>. A systematic survey of microbial communities associated with different sizes of particles is required to better understand microbial driven biogeochemical cycles in this specific system. Here we carried out a monthly microbial sampling starting from April 2015 for eight months at two stations, in the bay (station A53) and the connected open Yellow Sea (station D710) (Fig. S1). Detailed sample metadata including environmental factors can be found in the supplementary Table 1. Seawater samples were consecutively filtered through three pore-sized filters to collect microorganisms colonizing in the corresponding fractions (Fig. 1). After DNA extraction, samples collected in September 2015 and March 2016 were subjected to metagenomic sequencing, and samples collected in the first 8 months were subjected to amplicon sequencing (Fig. 1). Eukaryotic phytoplankton as approximated by chloroplast 16S rDNA sequences dominated the  $>2.7\ \mu\text{m}$  size fraction (11%–76%), though cyanobacteria (mainly *Synechococcus*) could occasionally accounted for :17% of all 16S rDNA reads in late summer (Fig. 2a). Alphaproteobacteria and Gammaproteobacteria were two most abundant phyla in the  $<2.7\ \mu\text{m}$  size fractions (Fig. 2a). Bacteroidota and Actinobacteriota dominated the 0.7–0.22  $\mu\text{m}$  fraction, each accounting for 4.7%–26% and 3.5%–23% of total amplicon reads on average, respectively (Fig. 2a). Although one should realize that the filtration cutoff does not provide an exact size exclusion since smaller microbes could be clogged in filters of the larger fraction, here microbial communities could be mainly partitioned into three clusters corresponding to the size fraction they primarily occupied as shown in the NMDS analysis (Fig. 2b). And all the three clusters were significantly influenced by temperature, Chl-*a*, and TN (total nitrogen) ( $p < 0.05$ , Fig. 2b).

Metagenomes were both assembled individually or co-assembled for each size fraction, and 915 non-redundant and purified environmental metagenomic-assembled genomes (MAGs) with  $\geq 50\%$  completeness and  $\leq 5\%$  contamination were obtained (Supplementary Table 3: MAGs info.), comprising 27 bacterial and 5 archaeal phyla (Figs. 3, 4). Among these MAGs, 469 have a completeness score of  $\geq 75\%$ , and 183 are near complete ( $\geq 90\%$ ). Bacterial MAGs were mainly from Proteobacteria (247 MAGs belonging to 20 orders of Alphaproteobacteria and 267 MAGs belonging to 21 orders of Gammaproteobacteria), Bacteroidota (179 MAGs out of 8 orders), and Actinobacteriota (57 MAGs out of 8 orders) (Fig. 3). Archaeal MAGs were mainly Marine Group II archaea (MGII), include 17 MGIIa MAGs and 3 MGIIb MAGs (Fig. 4). All the 14 MAGs of Cyanobacteriota are in the order of Synechococcales A, 11 of them are *Synechococcus*, and 3 are *Cyanobium*.

This monthly microbial survey at two contrasting stations provides a comprehensive and valuable database for studying microbial community succession and nutrient cycling of coastal marine environments.

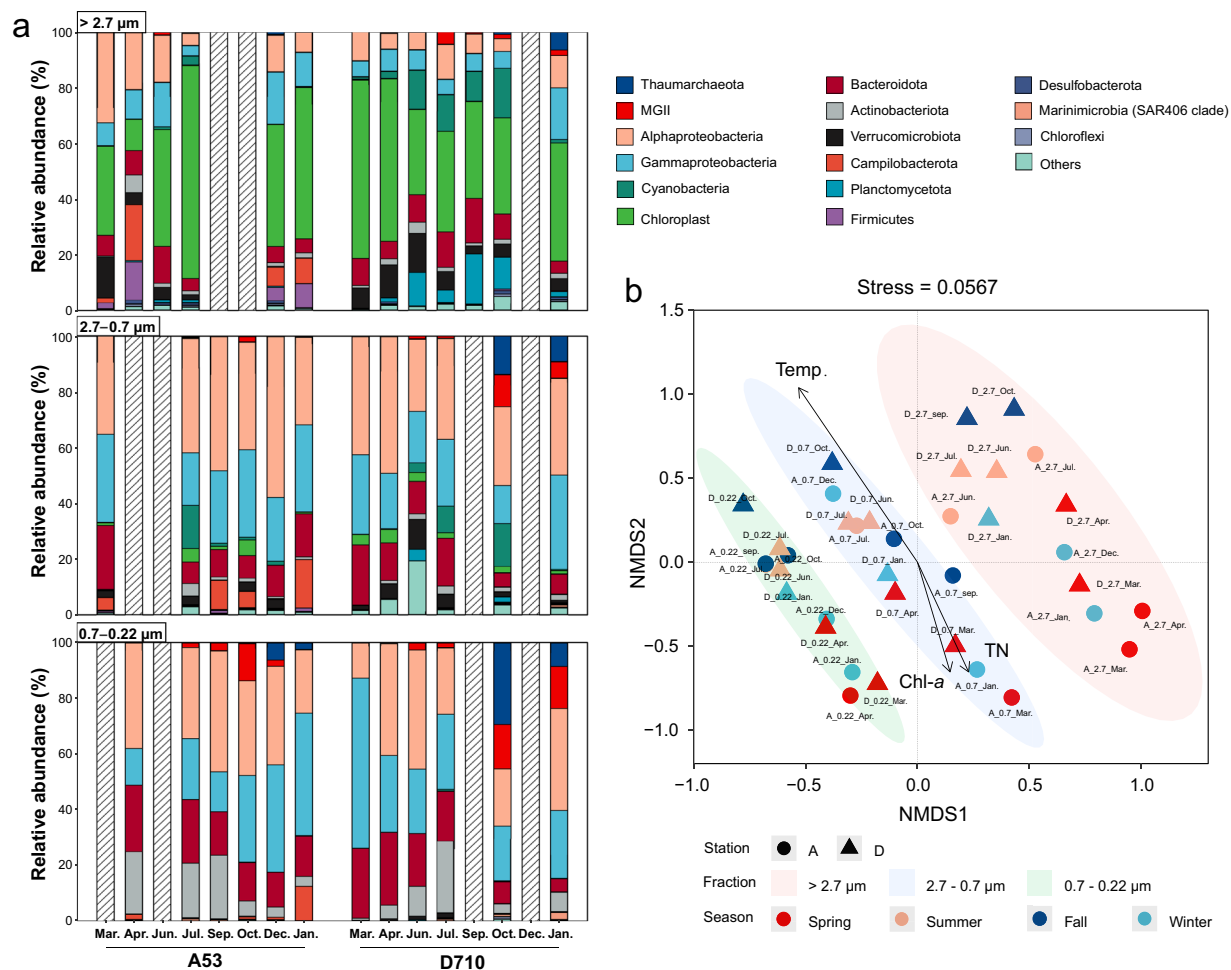


**Fig. 2** Relative abundance of ASVs in three size fractions **(a)** and NMDS ordination of samples based on Bray-Curtis dissimilarity matrix **(b)**. ASVs were color-coded according to their phyla, and those with total relative abundances of <5% in all 37 samples were grouped into Others. Hatched bars represent missing samples. Environmental factors were fit to the ordination using the envfit function in the vegan R package. Only factors with a significance level of <0.05 were shown. Detailed abundance data can be found in Supplementary Table 2, and associated environmental factors can be found in Supplementary Table 1.

## Methods

**Sampling and physicochemical analyses.** Samples were collected at two stations (Fig. S1) in 2015 (April, June, July, September, and December) and 2016 (January, March, and October) in JZB and the Yellow Sea on the “Innovation” research vessel operated by the Institute of Oceanography, Chinese Academy of Sciences. Microbial cells were collected onto three different pore-sized filters, e.g., 2.7  $\mu\text{m}$  (Whatman GF/D 1823-047), 0.7  $\mu\text{m}$  (Whatman GF/F 1825-047) and 0.22  $\mu\text{m}$  (Millipore GTTP04700), by sequentially filtering 4-L seawater collected at 0.5 m depth using a CTD sampler (Sea-Bird). Additionally, 1-L seawater was directly filtered through a 0.7  $\mu\text{m}$  pore-sized filter for particulate organic carbon (POC) measurement using a Shimadzu TOC-VCPH analyzer, and 50-ml seawater was sampled to measure the concentrations of dissolved organic carbon (DOC) and total nitrogen (TN) using a Shimadzu TOC-L Analyzer<sup>23</sup>. All filters and water samples were stored at  $-20^{\circ}\text{C}$ . Environmental parameters, including water temperature, salinity, and Chl-*a* concentration, were measured by the conductivity-temperature-depth (CTD) probe on board. Concentrations of specific nutrients, including the total nitrate,  $\text{NO}_2^-$ ,  $\text{PO}_4^{3-}$ ,  $\text{SiO}_3^{2-}$ , and  $\text{NH}_4^+$ , were measured using a SEAL AutoAnalyzer 3 automatic continuous flow analyzer in the lab.

**DNA extraction and metagenomic sequencing.** Samples taken in September 2015 and March 2016 were also selected for metagenomic sequencing to investigate microbial community disturbances during marine aquaculture farming and spring algal blooms. DNA was extracted for filter samples taken from the two months using FastDNA SPIN for soil kit (MP Biomedicals, LLC) according to the user manual. DNA materials were then sheared by a Covaris M220 Focused-ultrasonicator (Covaris, Woburn, MA, United States), and the resulting ~350 bp long fragments were further purified using MinkaGene Gel Extraction Kit (mCHIP, Guangzhou, China). Illumina libraries were constructed from about 100 ng DNA using NEB Next UltraTM DNA Library Prep Kit for Illumina (New England Biolabs, United States) according to the manufacturer’s instructions. Sequencing

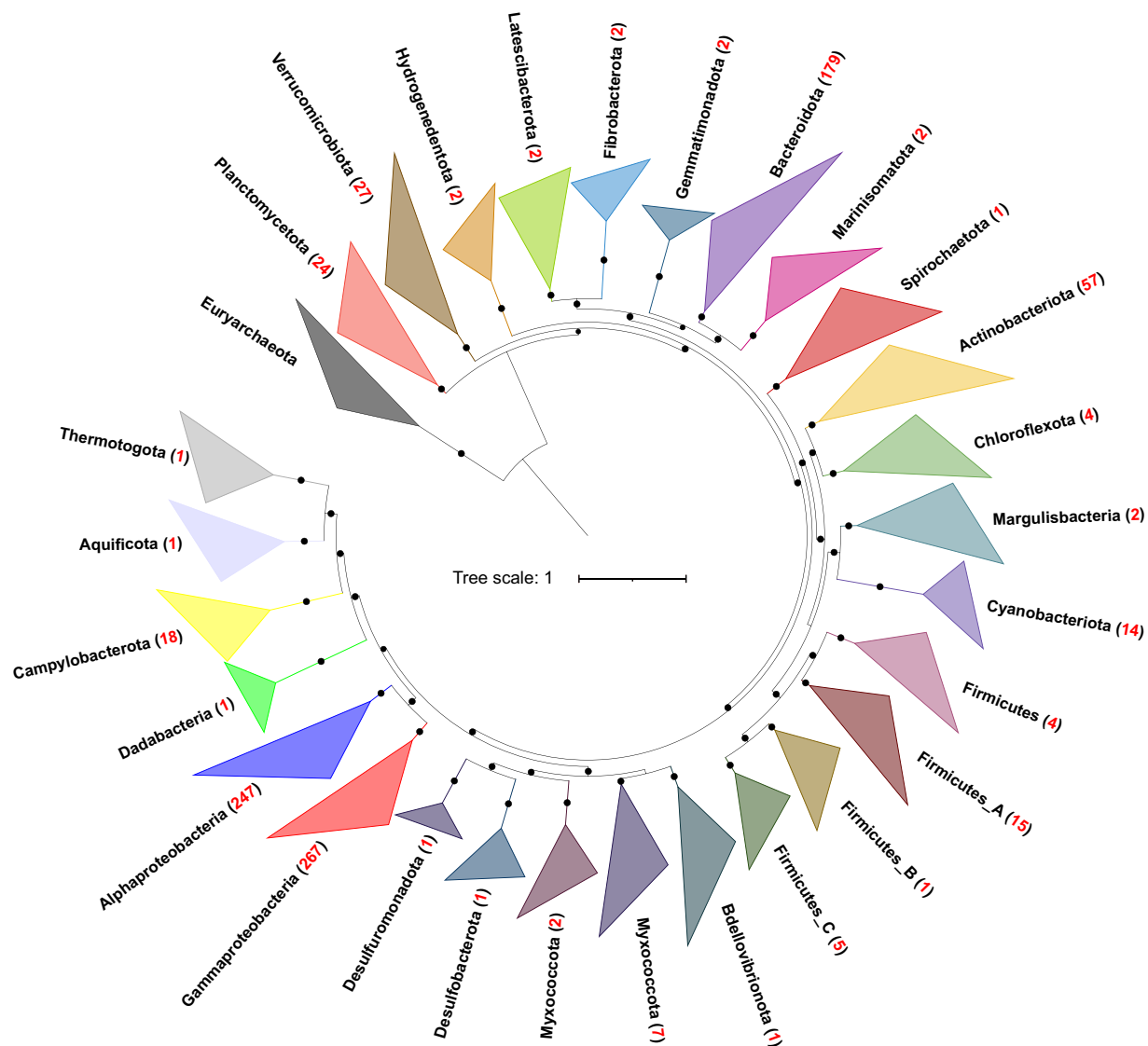


**Fig. 3** Phylogenomic placement of JZB bacterial MAGs. The maximum likelihood tree was reconstructed based on the concatenated alignments of 119 single-copy marker genes extracted from 890 JZB bacterial MAGs and 2656 reference genomes. The total number of MAGs recovered for each phylum was given in the parenthesis after the phylum name. Nodes with bootstrap values  $>0.5$  were labeled in the dendrogram using filled black circles with sizes proportional to the validity from 0.5 to 1. Five archaeal genomes in the Euryarchaeota phylum were used as the outgroup to root the tree. Detailed MAG taxonomy assignment, associated with completeness and contamination information can be found in Supplementary Table 3.

was performed on an Illumina HiSeq X-Ten platform using the  $2 \times 150$  bp paired-end chemistry at Magigene Biotechnology (Guangzhou, China).

**16S rDNA sequencing.** The V4 variable regions of 16S rDNA were amplified for 37 samples using the pair of universal prokaryotic primers 515FB (GTGYCAGCMGCCGCGGTAA) and 806RB (GGACTACNVGGGTWCTAAT)<sup>24</sup>. The PCR mixture contained 25  $\mu$ l of  $2 \times$  Premix Taq DNA polymerase (TaKaRa), 0.2 mM of each primer, 20  $\mu$ l of ddH<sub>2</sub>O, and 3  $\mu$ l of template DNA in a total volume of 50  $\mu$ l. Thermocycling steps were as follows: an initial denaturation step for 30 s at 94  $^{\circ}$ C, followed by 30 amplification cycles of 94  $^{\circ}$ C for 30 s, 58  $^{\circ}$ C for 30 s and 72  $^{\circ}$ C for 30 s, and a final elongation step at 72  $^{\circ}$ C for 30 s. Indexed PCR products were pooled and purified using the EZNA Gel Extraction Kit (Omega, USA) to remove primer dimers, and sequenced on the MiSeq platform ( $2 \times 300$  PE, Illumina) at MajorBio Biotechnology (Shanghai, China). Raw reads were analyzed using the Quantitative Insights into Microbial Ecology (QIIME2, version 2020.8) software suite with the demux, DADA2 and feature-table plugins<sup>25</sup>. Features with a total abundance of less than 10 across all samples, or those only present in one sample were discarded. Since sequencing depth was sufficient (Fig. S2), we subsampled the sequencing depth to the minimum sequence number of all samples, and reported a final ASV (Amplicon Sequence Variant) abundance table

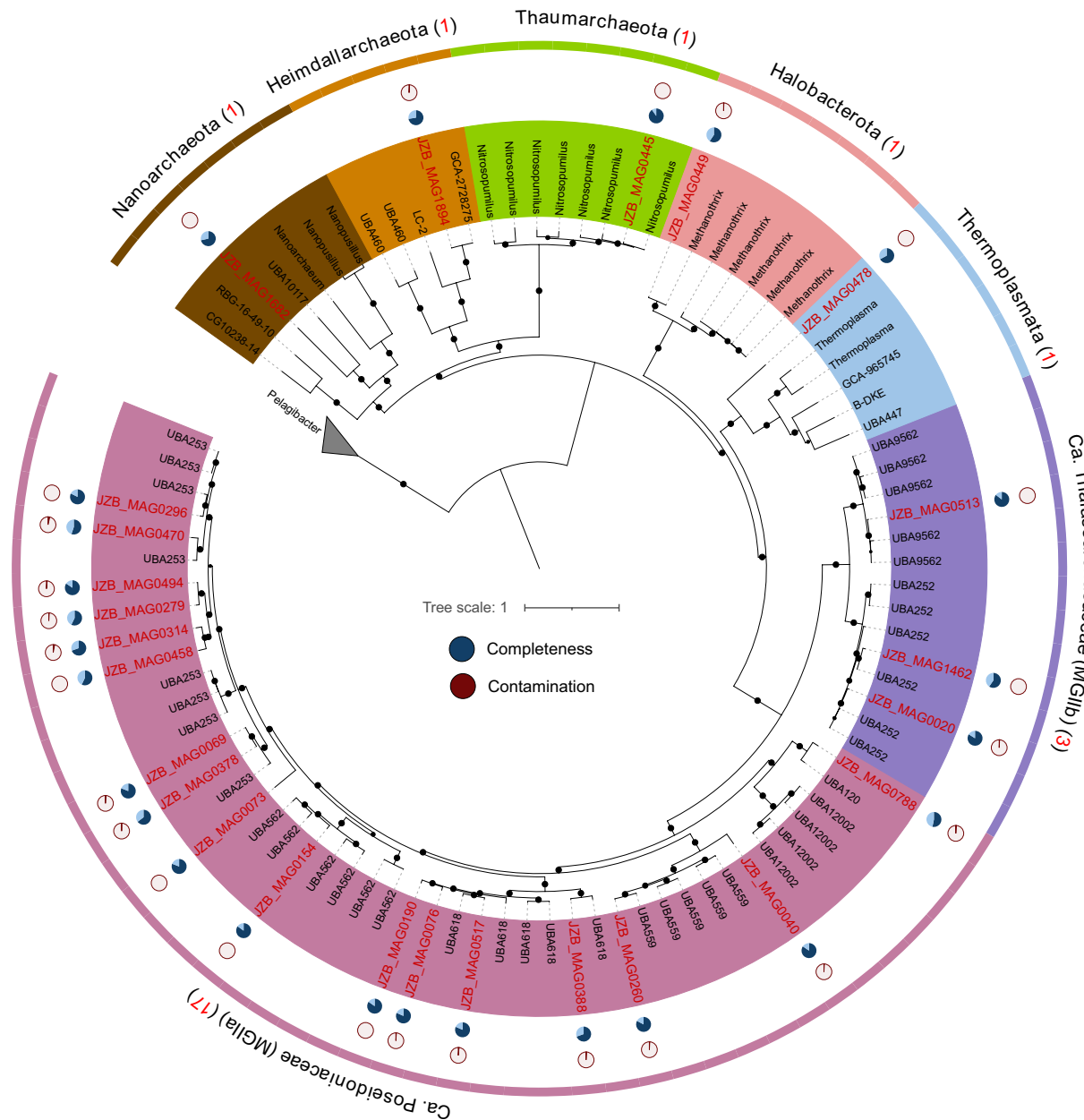


**Fig. 4** Phylogenomic placement of JZB archaeal MAGs with completeness and contamination information. The maximum likelihood tree was reconstructed based on the concatenated alignments of 117 single-copy marker genes extracted from 25 JZB archaeal MAGs (in red) and 68 reference genomes (in black). The total number of MAGs recovered for each phylum was given in the parenthesis after the phylum name. Nodes with bootstrap values  $>0.5$  were labeled in the dendrogram using filled black circles with sizes proportional to the validity from 0.5 to 1. Five *Pelagibacter* genomes were used as the outgroup to root the tree. Detailed MAG taxonomy assignment, associated with completeness and contamination information can be found in Supplementary Table 3.

with an even depth across samples (Supplementary Table 2). ASV taxonomy was assigned by the feature-classifier plugin using Naive Bayes against the SILVA v138 99% dereplicated reference database (<https://www.arb-silva.de/ngs>).

**Microbial community clustering analysis.** Non-metric multidimensional scaling (NMDS) based on Bray-Curtis distance was used to compare the differences in microbial community composition across samples, and environmental factors were fitted to the NMDS axes using the envfit method with 999 Monte Carlo tests using the vegan R package. Only factors with a significance level of  $<0.05$  were included in the NMDS figure (Fig. 2b).

**Sequence quality control and metagenomic assembly.** HiSeq generated raw reads were first trimmed by Trim Galore v0.5 using default settings to remove adaptors and low quality (below Q20) regions, and the final read quality was assessed using FastQC v0.11.8. Trimmed reads longer than 20 bp were used as clean reads for

downstream analyses. All 10 metagenomic samples collected in September 2015 and March 2016 were assembled individually using megahit v.1.1.3<sup>26</sup>, with the following parameters:—presets meta-sensitive and—min-count 1—k-list 25, 29, 39, 49, 59, 69, 79, 89, 99, 109, 119, 129, 141. In addition, a co-assembly step was done for samples from the same size fraction. Final assemblies were evaluated using Quast v.4.6.3<sup>27</sup>.

**MAG generation, refinement, purification, and taxonomy assignment.** Individually assembled and co-assembled contigs longer than 1 kb were subjected to metagenomic binning using BASALT<sup>28</sup>, which employed MetaBAT v2.12.1<sup>29</sup>, Maxbin v2.2.4<sup>30</sup> and CONCOCT v1.1.0<sup>31</sup> to make original bins, then compared these raw bins across assemblies to obtain a set of refined non-redundant MAGs. In addition, these MAGs were further refined using MAGpurify v2.12<sup>32</sup> to remove contaminations using the “phylo-markers”, “tetra-freq”, “gc-content”, “known-contam” and “clade-markers” modules. Genome quality was assessed using CheckM v1.0.11<sup>33</sup> and MAGs with completeness higher than 50% and contamination lower than 5% were further dereplicated using dRep v2.6.2<sup>34</sup> at 98% identity. The quality of MAGs was assessed by prok-quality<sup>35</sup> following the MIMAG standards<sup>36</sup>. Taxonomies of dereplicated MAGs were assigned using GTDB-Tk v0.1.6 based on the GTDB v86 database<sup>37,38</sup>.

**Phylogenomic tree construction.** Universal bacterial or archaeal single-copy marker genes used by the GTDBtk v1.7 were identified and extracted from both JZB MAGs and closest relative genomes in the GTDB v89 database. Only marker genes found in  $\geq 30$  genomes were selected to build the bacterial and archaeal phylogenomic trees. Protein sequences of selected marker genes were first aligned using MUSCLE (v3.8.31)<sup>39</sup>, and then trimmed using trimAl (v1.4)<sup>40</sup> with the “-automated1” option. The concatenated alignment sequences were used as the input of FastTree v2.1.1<sup>41</sup> to build phylogenomic trees with the “-gamma-lg” option. And the resulting trees were visualized using iTOL online server (<https://itol.embl.de>).

### Data Records

Raw reads of 16S rDNA and metagenome generated in this study have been deposited in the National Center for Biotechnology Information BioProject database with the project ID PRJNA823870<sup>42</sup> and PRJNA823908<sup>43</sup>. Contigs, MAGs and supplementary files have been deposited at figshare<sup>44</sup>.

### Technical Validation

All raw data processing steps, software and parameters used in this study were described in the Methods section. The quality of the genomes was also assessed by CheckM, and genomic statistics can be found in the supplementary tables.

### Code availability

All versions of third-party software and scripts used in this study are described and referenced accordingly in the Methods sections for ease of access and reproducibility.

Received: 21 June 2022; Accepted: 28 September 2022;

Published: 7 October 2022

### References

- Cavicchioli, R. *et al.* Scientists’ warning to humanity: microorganisms and climate change. *Nature Reviews Microbiology* **17**, 569–586 (2019).
- Azam, F. *et al.* The ecological role of water-column microbes in the sea. *Marine Ecology Progress Series* **10**, 257–263 (1983).
- Jiao, N. *et al.* Microbial production of recalcitrant dissolved organic matter: long-term carbon storage in the global ocean. *Nature Reviews Microbiology* **8**, 593–599 (2010).
- Zhang, C. *et al.* Evolving paradigms in biological carbon cycling in the ocean. *National Science Review* **5**, 481–499 (2018).
- Mestre, M. *et al.* Sinking particles promote vertical connectivity in the ocean microbiome. *Proceedings of the National Academy of Sciences* **115**, E6799–E6807 (2018).
- Baumas, C. M. J. *et al.* Mesopelagic microbial carbon production correlates with diversity across different marine particle fractions. *The ISME Journal* **15**, 1695–1708 (2021).
- Ortega-Retuerta, E., Joux, F., Jeffrey, W. H. & Ghiglione, J. F. Spatial variability of particle-associated and free-living bacterial diversity in surface waters from the Mackenzie River to the beaufort sea (canadian arctic). *Biogeosciences* **10**, 2747–2759 (2013). BG.
- Ganesh, S., Parris, D. J., DeLong, E. F. & Stewart, F. J. Metagenomic analysis of size-fractionated picoplankton in a marine oxygen minimum zone. *The ISME Journal* **8**, 187–211 (2014).
- Chen, S. *et al.* Interactions between marine group ii archaea and phytoplankton revealed by population correlations in the northern coast of south china sea. *Frontiers in Microbiology* **12** (2022).
- Eloe, E. A. *et al.* Compositional differences in particle-associated and free-living microbial assemblages from an extreme deep-ocean environment. *Environmental Microbiology Reports* **3**, 449–458 (2011).
- Salazar, G. *et al.* Particle-association lifestyle is a phylogenetically conserved trait in bathypelagic prokaryotes. *Mol Ecol* **24**, 5692–706 (2015).
- Karner, M. & Herndl, G. J. Extracellular enzymatic activity and secondary production in free-living and marine-snow-associated bacteria. *Marine Biology* **113**, 341–347 (1992).
- Grossart, H.-P., Tang, K. W., Kiorboe, T. & Ploug, H. Comparison of cell-specific activity between free-living and attached bacteria using isolates and natural assemblages. *FEMS Microbiology Letters* **266**, 194–200 (2007).
- Fierer, N. *et al.* Comparative metagenomic, phylogenetic and physiological analyses of soil microbial communities across nitrogen gradients. *The ISME Journal* **6**, 1007–1017 (2012).
- Leff, J. W. *et al.* Consistent responses of soil microbial communities to elevated nutrient inputs in grasslands across the globe. *Proceedings of the National Academy of Sciences* **112**, 10967–10972 (2015).
- Chen, Y. *et al.* Large amounts of easily decomposable carbon stored in subtropical forest subsoil are associated with *r*-strategy-dominated soil microbes. *Soil Biology and Biochemistry* **95**, 233–242 (2016).

17. Hou, S. *et al.* Benefit from decline: the primary transcriptome of *Alteromonas macleodii* str. Te101 during *Trichodesmium* demise. *The ISME Journal* **12**, 981–996 (2018).
18. Cleveland, C. C., Nergut, D. R., Schmidt, S. K. & Townsend, A. R. Increases in soil respiration following labile carbon additions linked to rapid shifts in soil microbial community composition. *Biogeochemistry* **82**, 229–240 (2007).
19. Ho, A., Di Lonardo, D. P. & Bodelier, P. L. E. Revisiting life strategy concepts in environmental microbial ecology. *FEMS Microbiology Ecology* **93** (2017).
20. Xing, J. *et al.* Fluxes, seasonal patterns and sources of various nutrient species (nitrogen, phosphorus and silicon) in atmospheric wet deposition and their ecological effects on Jiaozhou Bay, North China. *Sci Total Environ* **576**, 617–627 (2017).
21. Zhang, L., Xiong, L., Li, J. & Huang, X. Long-term changes of nutrients and biocenoses indicating the anthropogenic influences on ecosystem in Jiaozhou Bay and Daya Bay, China. *Mar Pollut Bull* **168**, 112406 (2021).
22. Zhang, X. *et al.* Effects of organic nitrogen components from terrestrial input on the phytoplankton community in Jiaozhou Bay. *Marine Pollution Bulletin* **174**, 113316 (2022).
23. Sharp, J. *et al.* Final dissolved organic carbon broad community intercalibration and preliminary use of DOC reference materials. *Marine Chemistry* **77** (2002).
24. Walters, W. *et al.* Improved bacterial 16S rRNA gene (V4 and V4-5) and fungal internal transcribed spacer marker gene primers for microbial community surveys. *mSystems* **1** (2016).
25. Bolyen, E. *et al.* Reproducible, interactive, scalable and extensible microbiome data science using QIIME 2. *Nature Biotechnology* **37**, 852–857 (2019).
26. Li, D. *et al.* MEGAHIT v1.0: A fast and scalable metagenome assembler driven by advanced methodologies and community practices. *Methods* **102**, 3–11 (2016).
27. Mikheenko, A., Saveliev, V. & Gurevich, A. MetaQUAST: evaluation of metagenome assemblies. *Bioinformatics* **32**, 1088–90 (2016).
28. Yu, K. *et al.* Recovery of high-quality genomes from a deep-inland salt lake using BASALT. *bioRxiv* <https://doi.org/10.1101/2021.03.05.434042> (2021).
29. Kang, D. D. *et al.* MetaBAT 2: an adaptive binning algorithm for robust and efficient genome reconstruction from metagenome assemblies. *PeerJ* **7**, e7359 (2019).
30. Wu, Y. W., Simmons, B. A. & Singer, S. W. MaxBin 2.0: an automated binning algorithm to recover genomes from multiple metagenomic datasets. *Bioinformatics* **32**, 605–7 (2016).
31. Alneberg, J. *et al.* Binning metagenomic contigs by coverage and composition. *Nat Methods* **11**, 1144–6 (2014).
32. Nayfach, S. *et al.* New insights from uncultivated genomes of the global human gut microbiome. *Nature* **568** (2019).
33. Parks, D. H., Imelfort, M., Skennerton, C. T., Hugenholtz, P. & Tyson, G. W. CheckM: assessing the quality of microbial genomes recovered from isolates, single cells, and metagenomes. *Genome Res* **25**, 1043–55 (2015).
34. Olm, M. R., Brown, C. T. & Banfield, J. F. dRep: a tool for fast and accurate genomic comparisons that enables improved genome recovery from metagenomes through de-replication. *The ISME Journal* **5** (2017).
35. Albanese, D. & Donati, C. Large-scale quality assessment of prokaryotic genomes with metashot/prok-quality. *F1000Research* **10** (2021).
36. Bowers, R. M. *et al.* Minimum information about a single amplified genome (misag) and a metagenome-assembled genome (mimag) of bacteria and archaea. *Nature Biotechnology* **35**, 725–731 (2017).
37. Parks, D. H. *et al.* A complete domain-to-species taxonomy for bacteria and archaea. *Nat Biotechnol* **38**, 1079–1086 (2020).
38. Chaumeil, P. A., Mussig, A. J., Hugenholtz, P. & Parks, D. H. GTDB-Tk: a toolkit to classify genomes with the genome taxonomy database. *Bioinformatics* (2019).
39. Edgar, R. C. MUSCLE: multiple sequence alignment with high accuracy and high throughput. *Nucleic Acids Res* **32**, 1792–7 (2004).
40. Capella-Gutierrez, S., Silla-Martinez, J. M. & Gabaldon, T. trimAl: a tool for automated alignment trimming in large-scale phylogenetic analyses. *Bioinformatics* **25**, 1972–3 (2009).
41. Price, M. N., Dehal, P. S. & Arkin, A. P. FastTree 2—approximately maximum-likelihood trees for large alignments. *PLoS one* **25**, e9490–e9490 (2010).
42. NCBI Sequence Read Archive <https://identifiers.org/ncbi/insdc.sra:SRP367774> (2022).
43. NCBI Sequence Read Archive <https://identifiers.org/ncbi/insdc.sra:SRP367809> (2022).
44. Tao, J. Jiaozhou bay 16S rDNA & metagenome dataset. *figshare* <https://doi.org/10.6084/m9.figshare.19690459.v6> (2022).

## Acknowledgements

This study was supported by the Southern Marine Science and Engineering Guangdong Laboratory (Guangzhou) (No. K19313901), the National Natural Science Foundation of China (Nos. 42276163, 91851210, 42141003), the State Key R&D project of China grant (No. 2018YFA0605800), the Shenzhen Key Laboratory of Marine Archaea Geo-Omics, Southern University of Science and Technology (SUSTech) (ZDSYS201802081843490), and the Stable Support Plan Program of Shenzhen Natural Science Fund (20200925173954005). S. Hou was also supported by the MEL Visiting Fellowship of Xiamen University (Grant ID: MELRS2210). Computation in this study was supported by the SUSTech Centre for Computational Science and Engineering.

## Author contributions

S.H. and C.Z. conceived this study. J.T. conducted field sampling and DNA extraction. J.T. and W.W. analyzed the amplicon data, assembled the metagenomes, generated the MAGs and produced all figures under the supervision of S. H. and C.Z. J.T. and S.H. interpreted the results and wrote the first draft. S.H., C.Z. and J.L.W. revised the draft. All authors reviewed and contributed to the final version of the manuscript.

## Competing interests

The authors declare no competing interests.

## Additional information

**Supplementary information** The online version contains supplementary material available at <https://doi.org/10.1038/s41597-022-01734-3>.

**Correspondence** and requests for materials should be addressed to S.H.

**Reprints and permissions information** is available at [www.nature.com/reprints](http://www.nature.com/reprints).

**Publisher's note** Springer Nature remains neutral with regard to jurisdictional claims in published maps and institutional affiliations.



**Open Access** This article is licensed under a Creative Commons Attribution 4.0 International License, which permits use, sharing, adaptation, distribution and reproduction in any medium or format, as long as you give appropriate credit to the original author(s) and the source, provide a link to the Creative Commons license, and indicate if changes were made. The images or other third party material in this article are included in the article's Creative Commons license, unless indicated otherwise in a credit line to the material. If material is not included in the article's Creative Commons license and your intended use is not permitted by statutory regulation or exceeds the permitted use, you will need to obtain permission directly from the copyright holder. To view a copy of this license, visit <http://creativecommons.org/licenses/by/4.0/>.

© The Author(s) 2022, corrected publication 2022